Assessment of Transmitted Power Density in the Planar Multilayer Tissue Model due to Radiation from Dipole Antenna

Dragan Poljak, Anna Šušnjara and Ana Fišić

Original scientific article

***Abstract*—Recent relevant safety guidelines IEEE-Std C95.1-2019 and ICNIRP-RF Guidelines 2020 have converged towards 6 GHz as a transition frequency from specific absorption rate (*SAR*), as basic restriction quantity, to absorbed power density (*APD*). Namely, the penetration of electromagnetic waves into the human tissue rapidly decreases as frequency increases, therefore, tissue heating can be considered as superficial above 6 GHz. However, besides the *APD*, an alternative internal dosimetric quantity transmitted power density or *TPD* is sometimes computed since its relation to *SAR* is more obvious and is easier to obtain. This paper deals with an analytical/numerical approach to determine *TPD* in planar multi-layered model of the human tissue exposed to the dipole antenna radiation. Analytical approach deals with assumed sinusoidal current distribution, while numerical approach pertains to the determination of current by solving the corresponding Pocklington integro-differential equation via Galerkin-Bubnov Indirect Boundary Element Method. The novelty presented in this paper with respect to previous work is a multilayer geometry whose effects are considered via the corresponding Fresnel plane wave reflection/transmission approximation. Some illustrative results for current distribution, transmitted field, volume power density (*VPD*) and *TPD* at various frequencies and distances of the antenna from the interface are given.**

***Index terms*—analytical/numerical approach, current distribution, dipole antenna, planar multilayer tissue model, plane wave approximation.**

I. Introduction

Exposure of humans to millimeter waves generated by Fifth generation (5G) mobile communication systems has caused public concern regarding potential health hazard. Recent relevant safety guidelines; IEEE-Std C95.1-2019 [1] ICNIRP-RF Guidelines – 2020 [2] have converged towards 6 GHz as transition frequency from specific absorption rate (*SAR*), as basic restriction quantity, to absorbed power density (*APD*). Namely, above transition frequency, the use APD averaged over a control area is suggested in the near field region instead of SAR averaged over tissue volume [3], [4] and [5]. Also, instead of considering temperature elevation in a volume of tissue, related surface temperature elevation in the eye and skin is of interest (eye, skin, ear) as a relevant biological effect. An illustrative review on the subject could be found elsewhere, e.g., in [4].

On the other hand, a dosimetric quantity alternative to APD referred to as an area-averaged transmitted power density (*TPD*) at skin surface and metric convenient to address the surface temperature increase has also been used [6].

Some preliminary studies pertaining to a rather simplified assessment of *TPD* due the Hertz dipole radiating in the presence of a lossy medium featuring Fresnel coefficient approximation and Modified Image Theory (MIT) has been carried out in [7] and [8], respectively.

Furthermore, an extension of the Hertz dipole case presented in [7] and [8] to the dipole antenna radiating in front of homogeneous lossy medium (flat tissue with muscle properties) has been reported in [9] dealing with mathematical model for the assessment of parameters of interest and in [10] where some illustrative results for the transmitted field, volume power density (*VPD*) and *TPD* are given. Note that in [9] and [10] the antenna current is first assumed to be sinusoidal, while an alternative deals with a calculated current distribution governed by the Pocklington integro-differential equation for the wires above a homogeneous lossy half-space. Pocklington equation is handled numerically via Galerkin-Bubnov Indirect Boundary Element Method (GB-IBEM). Provided the current distribution along the dipole has been either assumed or numerically calculated, the field transmitted into the lossy medium representing the human tissue, *VPD* and *TPD* have been evaluated.

This work further extends the approach used in [9] and [10] by representing a tissue in terms of planar multilayer. The effect of multi-layered half-space is considered via the corresponding reflection/transmission coefficient already used in the analysis of ground penetrating radar (GPR) [11] and [12].

The paper is organized, as follows; First the integral equation formulation for the determination of the current distribution along the antenna radiating above a multilayer is outlined. Furthermore, the integral expressions for the transmitted field, *VPD* and *TPD* are given. Note that *TPD* is derived in Appendix. Section III deals with the results obtained by using the assumed and calculated current distribution, respectively.

Manuscript received October 19, 2022; revised January 16, 2022. Date of publication February 17, 2023. Date of current version February 17, 2023.

D. Poljak and A. Šušnjara are with the Department of Electronics and Computer Science, FESB, Univ. of Split, Croatia (e-mails: dpoljak@fesb.hr, ansusnja@fesb.hr). A. Fišić is with Ericsson Nikola Tesla d. d., Zagreb (email: Ana.Fisic00@fesb.hr).

Digital Object Identifier (DOI): 10.24138/jcomss-2022-0050

II. FORMULATION

Dipole antenna of radius *a* and length *L* horizontally located in front of a multi-layered planar tissue, as shown in Fig. 1, driven by a voltage source is considered.

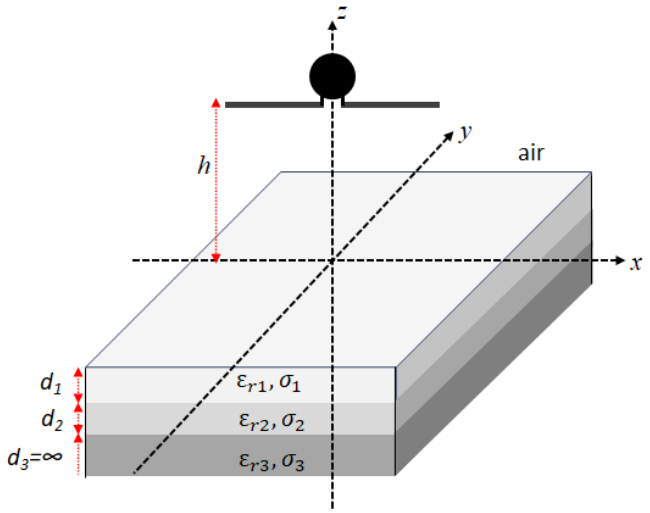

Fig. 1. Horizontal dipole antenna in front of a planar multi-layered tissue

A fundamental parameter in the analysis of antenna properties is the current distribution along the wire. Provided the current distribution is known the electric field transmitted into the tissue, volume power density (*VPD*) and transmitted power density (*TPD*) can be determined. As it is well-known from the wire antenna theory the current distribution along the dipole antenna is governed by the corresponding Pocklington integro-differential equation.

A. Current Distribution

The Pocklington integro-differential equation for thin wire above a multilayer can be written in the form [9]

$$E_x^{exc} = \frac{1}{j4\pi\omega\varepsilon_0}\left[\int_{-L/2}^{L/2} \frac{\partial I(x\prime)}{\partial x\prime}\frac{\partial g_a(\vec{r},x\prime)}{\partial x}dx' - k_0^2\int_{-L/2}^{L/2} I(x')g_a(\vec{r},x')dx'\right] \quad (1)$$

where $I(x')$ stands for current distribution along the wire, k_0 denotes the wave number of free space and the total Green function is

$$g_a(x,x') = g_{a0}(x,x') - \Gamma^{ref}(\theta')g_{ai}(x,x') \quad (2)$$

with the Green function of an unbounded lossless medium given by

$$g_a(x,x') = \frac{e^{-jkR_a}}{R_a} \quad (3)$$

while $g_{ai}(x,x')$ arises from the image theory:

$$g_{ai}(x,x') = \frac{e^{-jkR_{ai}}}{R_{ai}} \quad (4)$$

where R_a denotes the distance from the antenna axis to the observation point at the wire surface, while R_{ai} pertains to the image wire.

The influence of the interface air-multilayer is taken into account via the corresponding Fresnel plane wave reflection coefficient Γ^{ref} [11].

The assumed sinusoidal current distribution

$$I(x') = I_m \sin k_0\left(\frac{L}{2} - |x'|\right) \quad (5)$$

stems from the analytical solution of integro-differential equation (1) in free space under certain set of approximations [9].

On the other hand, a so-called exact current distribution can be obtained by numerically solving Pocklington equation (1). The numerical solution of (1) via Galerkin-Bubnov Indirect Boundary Element Method (GB-IBEM) has been reported elsewhere, e.g., in [13] and [14].

B. Electric Field Formulas

Provided the current distribution is known, either assumed or calculated, the components of the electric field transmitted in the multilayer tissue model are [10]:

$$E_x(\vec{r}) = \frac{1}{j4\pi\omega\varepsilon_{eff}}\left[\int_{-L/2}^{L/2} \frac{\partial I(x\prime)}{\partial x\prime}\frac{\partial g(\vec{r},x\prime)}{\partial x}dx' - \gamma^2\int_{-L/2}^{L/2} I(x')g(\vec{r},x')dx'\right] \quad (6)$$

$$E_y(\vec{r}) = \frac{1}{j4\pi\omega\varepsilon_{eff}}\int_{-L/2}^{L/2} \frac{\partial I(x\prime)}{\partial x\prime}\frac{\partial g(\vec{r},x\prime)}{\partial y}dx' \quad (7)$$

$$E_z(\vec{r}) = \frac{1}{j4\pi\omega\varepsilon_{eff}}\int_{-L/2}^{L/2} \frac{\partial I(x\prime)}{\partial x\prime}\frac{\partial g(\vec{r},x\prime)}{\partial z}dx' \quad (8)$$

where ε_{eff} is the complex permittivity of the ground while γ is the complex propagation constant of a lossy medium (the human tissue)

$$\gamma = \sqrt{(j\omega\mu\sigma - \omega^2\mu\varepsilon)} \quad (9)$$

The total Green function can be written in the form

$$g(\vec{r},x') = \Gamma^{tr}g_0(\vec{r},x') \quad (10)$$

where Green function of unbounded lossy medium is

$$g_0(\vec{r},x') = \frac{e^{-\gamma R}}{R} \quad (11)$$

where R_0 is the observation point distance from the antenna and Γ^{tr} is a plane wave transmission coefficient for multi-layered medium [12].

Evaluation of integrals (6)-(8) can be carried out by means of numerical integration combined with finite difference approximation of derivatives of the total Green function to treat quasi-singularity problems [13]. Furthermore, numerical computation of field integrals (6)-(8) using the numerically obtained current distribution via GB-IBEM is available elsewhere, e.g., in [13] and [14].

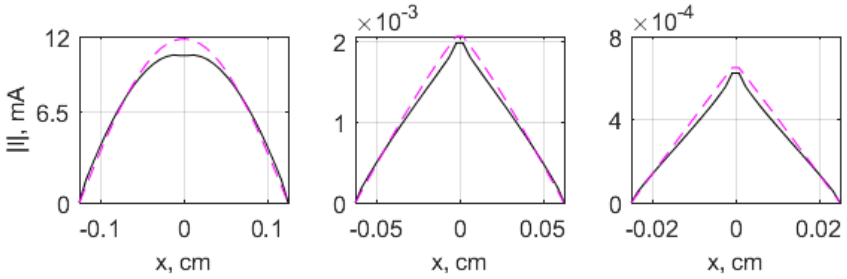

Fig. 2. Numerical (black) and analytical (magenta) solutions of current distribution along the antenna placed 1 cm above two-layered model. Antenna lengths are $L=\lambda/2$ (left), $\lambda/4$ (center) and $\lambda/10$ (right) and operating frequency is f=6 GHz.

C. Volume Power Density (VPD) and Transmitted Power Density (TPD)

The volume power density (*VPD*) in media with finite conductivity is given by:

$$VPD = \frac{1}{2}\sigma(\vec{r})|E(\vec{r})|^2 \tag{12}$$

The broadside field component is of interest, i.e., x=0, y=0 and z= (0,-∞), therefore, y component of electric field vanishes, [7] and [8]. Hence, eq. (12) can be written in the following form:

$$VPD = \frac{1}{2}\sigma(z)(|E_x(z)|^2 + |E_z(z)|^2) \tag{13}$$

Furthermore, the transmitted power density (*TPD*) is defined, as follows [6]

$$TPD = \frac{1}{2}\int_0^r \sigma(\vec{r})|E(\vec{r})|^2 dr \tag{14}$$

where r is the variable perpendicular to the surface of the human body and point r=0 refers to the air-body interface, while σ stands for a tissue conductivity.

For the geometry considered in this paper, depicted Fig 1, *TPD* is given by

$$TPD(z) = \frac{1}{2}\int_0^{z_{end}} \sigma(z)(|E_x(z)|^2 + |E_z(z)|^2) dz \tag{15}$$

where z_{end} stands for the tissue depth taken into account within the *TPD* calculation.

A complete derivation of *TPD* starting from the Poynting integral theorem is given in the Appendix.

III. Results

Computational examples are obtained using the two- and three-layered models, respectively. Illustrative results pertain to transmitted field, *VPD* and *TPD* for various distances of the wire from the interface, antenna lengths and frequencies. In all cases dipole antenna is excited by the unitary voltage source V_0=1 V and wire radius is chosen as $a=L/(10N)$, where N is a number of wire segments within GB-IBEM solution procedure.

Frequency dependent parameters of skin, fat and muscle tissues originating from Gabriels' compilation [15] and reported later in ITIS database [16] are given in Table 1.

TABLE I
Frequency dependent parameters of body tissues [16]

	Skin		Fat		Muscle	
f (GHz)	ε_r	σ (S/m)	ε_r	σ (S/m)	ε_r	σ (S/m)
6	34.9	3.89	9.80	0.872	48.2	5.20
10	31.3	8.01	8.80	1.71	42.8	10.6
30	15.5	27.1	5.91	5.33	23.2	35.5
60	7.98	36.4	4.40	8.39	12.9	52.8

A. Two-layer Model

Two-layer tissue model is characterized by layers of skin (d_1=1.5 mm) and muscle ($d_2+d_3=\infty$) (Fig. 1.). Dipole antenna is placed at distance h horizontally to the interface.

Fig. 2 shows the current distribution along the antenna at distance h=1 cm from the interface, compared with the assumed sinusoidal current distribution at f=6 GHz. The discrepancy between calculated and approximate sinusoidal current distribution appears in the feed-gap area. Considering all combinations of antenna heights, antenna lengths and frequencies, the maximal discrepancy is appx. 4.5%.

The next set of figures (Figs. 3-5) represents transmitted field, *VPD* and *TPD* for different values of antenna height, antenna lengths and various frequencies.

Electric (E) field decreases rapidly with tissue depth ($|E|$ vs. z). Increasing the antenna-body distance at fixed antenna length and frequency, the field decreases ($|E|$ vs. h). However, skin-depth does not depend on antenna-body distance. Namely, skin-depth is the distance from the air-body interface at which transmitted field falls to appx. 36% of its maximal value. Figs. 3-5 show that, no matter the antenna length, the skin-depth at 6 and 10 GHz is in muscle tissue, while at 30 and 60 GHz the skin-depth is in the skin tissue. Although the field increases with frequency ($|E|$ vs. f), the higher the frequency, the field approaches zero more rapidly. Also, E field decreases with antenna length ($|E|$ vs. L).

As for analytical and numerical approaches in the current solution, the difference that they introduce in the electric field computation is small and it tends to decrease as frequency and antenna length decrease.

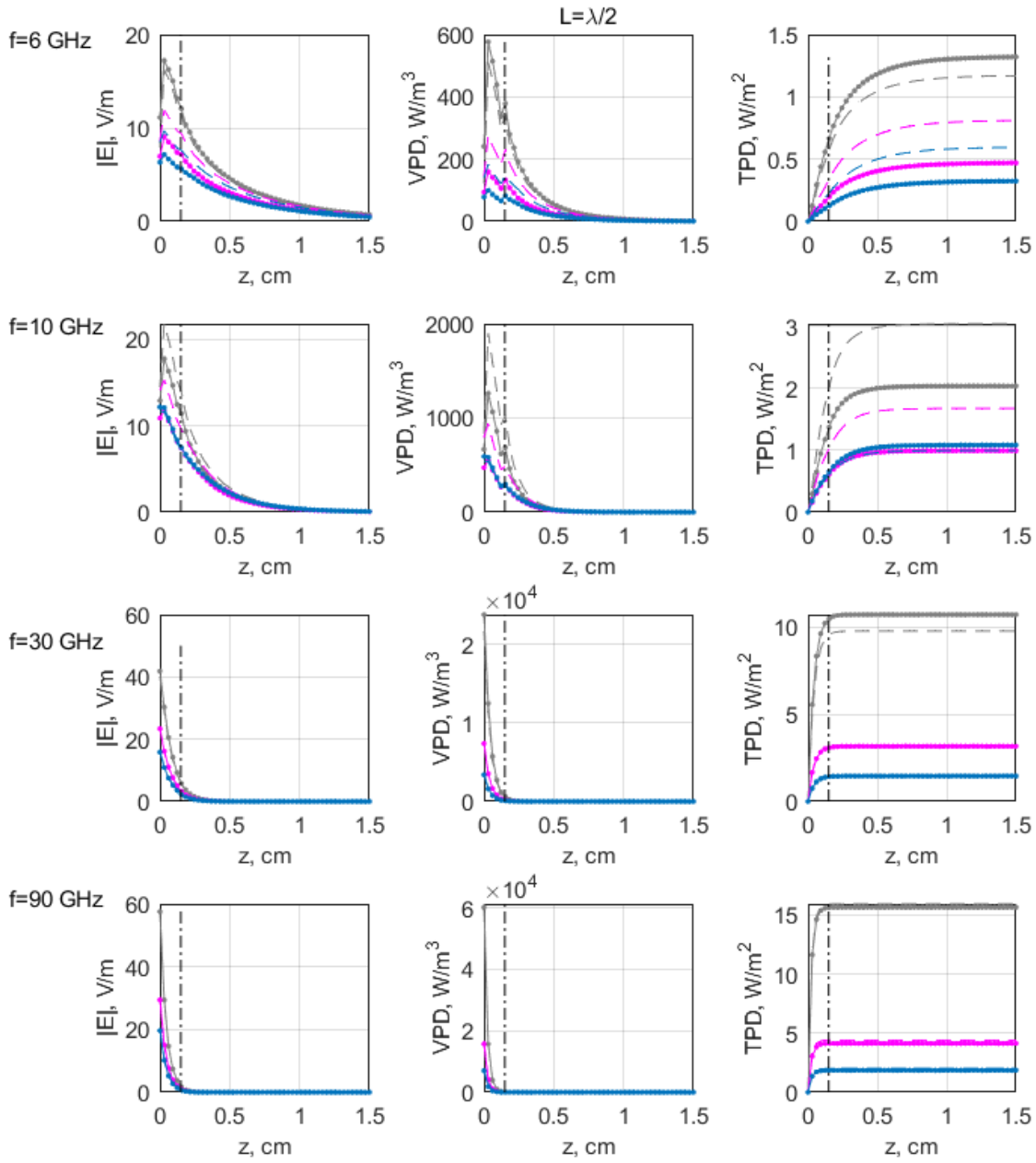

Fig. 3. Absolute value of electric field transmitted into the tissue (|*E*|, left), volume power density (*VPD*, center) and transmitted power density (*TPD*, right) vs. tissue depth for halfwave dipole ($L=\lambda/2$) above two-layered tissue.

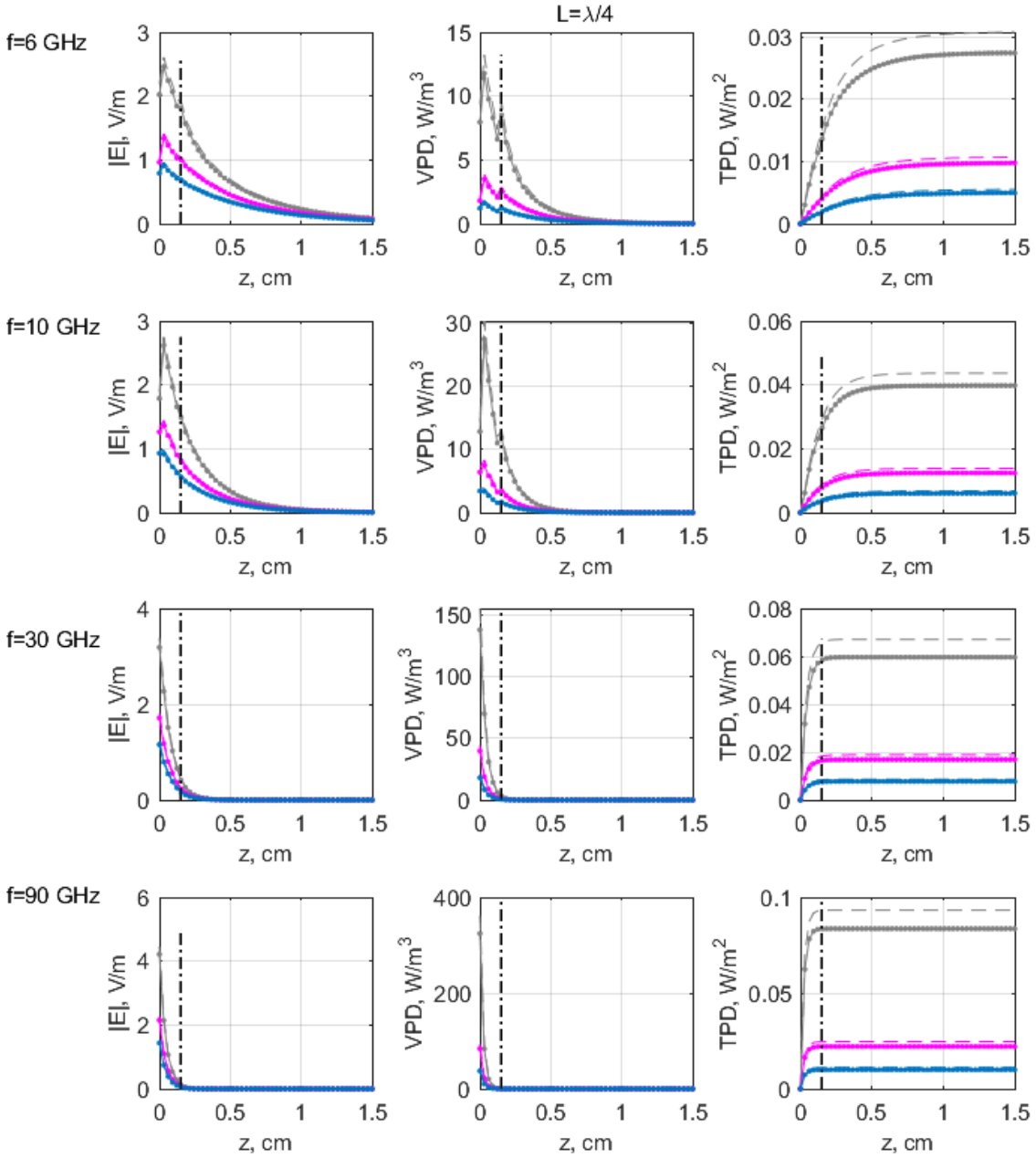

Fig. 4. Absolute value of electric field transmitted into the tissue (|*E*|, left), volume power density (*VPD*, center) and transmitted power density (*TPD*, right) vs. tissue depth for quarter-wavelength dipole ($L=\lambda/4$) above two-layered tissue.

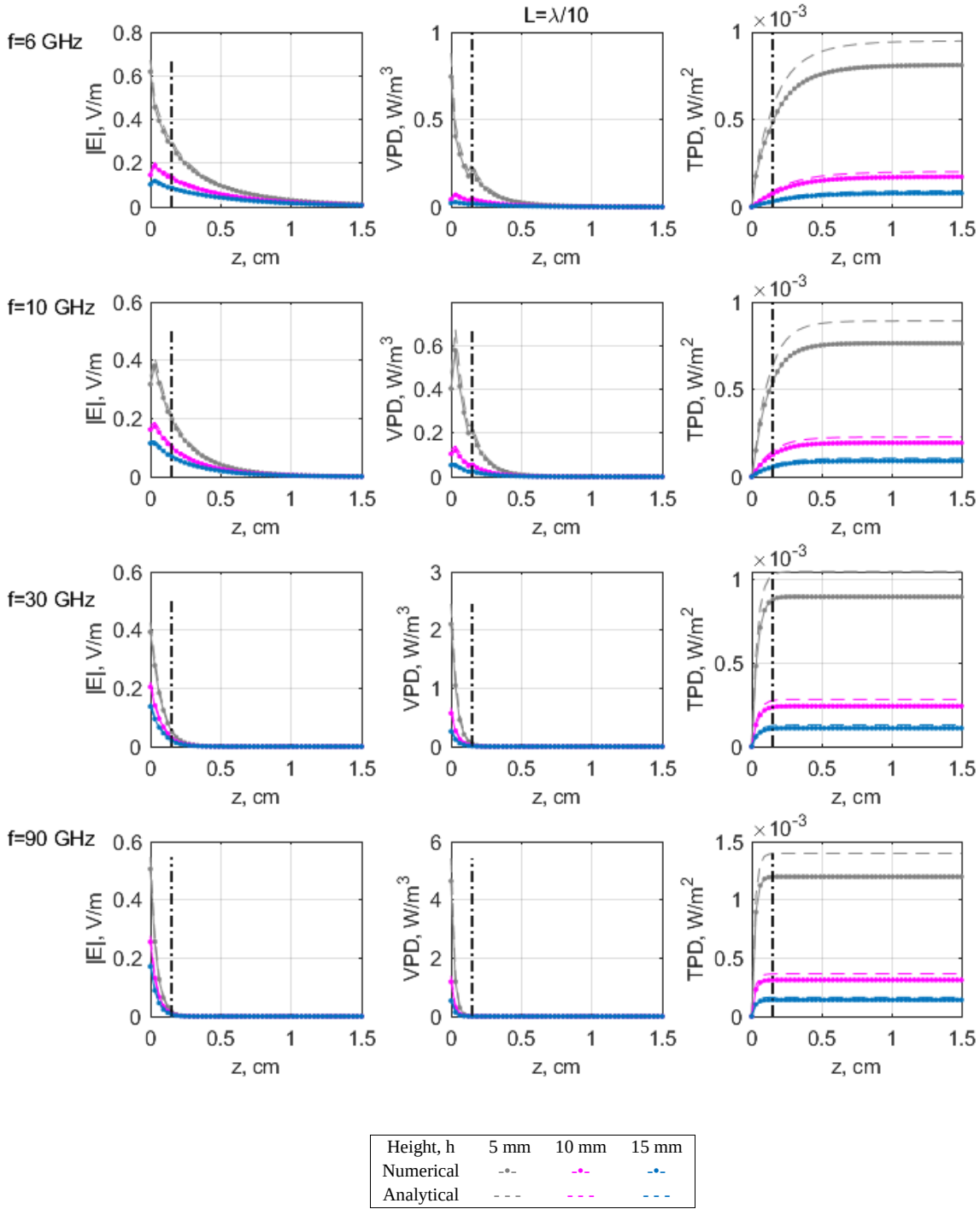

Fig. 5. Absolute value of electric field transmitted into the tissue (|*E*|, left), volume power density (*VPD*, center) and transmitted power density (*TPD*, right) vs. tissue depth for tenth-wavelength dipole ($L=\lambda/10$) above two-layered tissue.

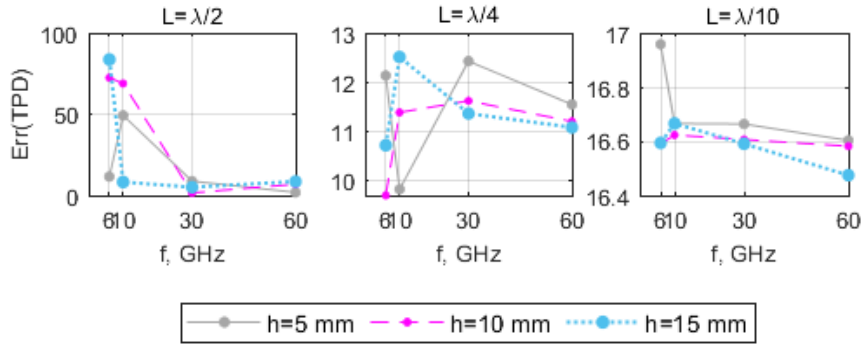

Fig. 6. Absolute relative error for *TPD* in two-layered body model computed as $Err(TPD) = |TPD_{num} - TPD_{ana}| / |TPD_{ana}|*100$. Subscripts *num* and *ana* denote *TPD* computed with numerical and analytical current solutions, respectively.

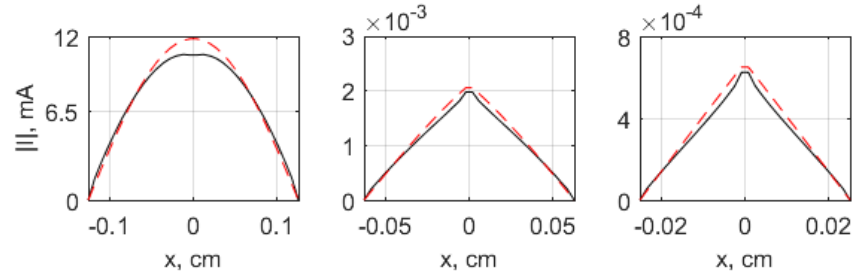

Fig. 7. Numerical (black) and analytical (red) solutions of current distribution along the antenna placed 1 cm above three-layered model. Antenna lengths are $L=\lambda/2$ (left), $\lambda/4$ (center) and $\lambda/10$ (right) and operating frequency is f=6 GHz.

Furthermore, *VPD* depends on antenna length, antenna-body distance, and frequency, in similar way as *E* field but with faster decay rate versus tissue depth. However, the discrepancy between the analytical and numerical approaches in *VPD* computation is more pronounced, although they still exhibit a good agreement.

Finally, *TPD* increases until saturation. The tissue depth at which *TPD* enters the saturation depends on frequency and tends to be closer to body surface as frequency increases. This is equivalent to the skin-depth frequency dependence.

Naturally, the discrepancy between analytical and numerical results is higher for *TPD* when compared with *E* field and *VPD*. In particular, the greatest discrepancies are found for $L=\lambda/2$, at 6 and 10 GHz. This difference decreases with antenna length. Generally, the smaller the antenna-body distance, the larger is the discrepancy between the analytical and numerical solutions. The relative absolute error between the analytical and numerical *TPD* solutions is depicted in Fig 6. It is worth noting that the error does not depend on tissue depth.

B. Three-layer Model

Three-layer tissue model consists of layers of skin (d_1=1.5 mm), fat (d_2=4 mm) and muscle ($d_3=\infty$) (Fig. 1.). Dipole antenna is placed at distance *h* horizontally to the interface.

The current distribution along the antenna at horizontal distance h=1 cm from the interface, compared with the assumed sinusoidal current distribution at f=6 GHz is depicted in Fig. 7. The maximal discrepancy, considering all combinations, appears in the feed gap area and it does not exceed 8%.

Figs. 8-10 show results for the transmitted *E* field, *VPD* and *TPD* for different values of antenna height, antenna length and various frequencies.

The maximal magnitude of *E* field occurs farther away from the air-body interface when compared to its position in two-layer model. Furthermore, the point at which the field reaches zero is located deeper inside the tissue. Due to reflections from skin-fat and fat-muscle interfaces, the distribution is characterized with three different regions. In the first region corresponding to skin, *E* field rises towards its maximal value which occurrs in the proximity of the skin-fat interface. After that, the field starts to decrease with slope narrower in the fat tissue (2nd region) than in the muscle tissue (3rd region). However, the difference in the distribution character between the regions tends to fade out as frequency increases. Also, as frequency increases, the maximal magnitude of *E* field moves closer to the air-skin interface and the slope of the field descent levels out in all tissues.

Furthermore, field values are somewhat lower at 6 and 10 GHz for the same antenna lengths when compared to two-layer model. Still, by increasing the frequency and antenna-body distance the difference in electric field magnitudes between the two models decreases.

Expectedly, *VPD* follows the *E* field distribution. *VPD* values are much higher in skin than in fat, while their magnitude in the muscle tissue rapidly approaches to zero in all cases.

As for *TPD*, the saturation-depth is different when compared to two-layer model at 6 and 10 GHz. Increasing the frequency, the difference between the two- and three-layer models becomes insignificant.

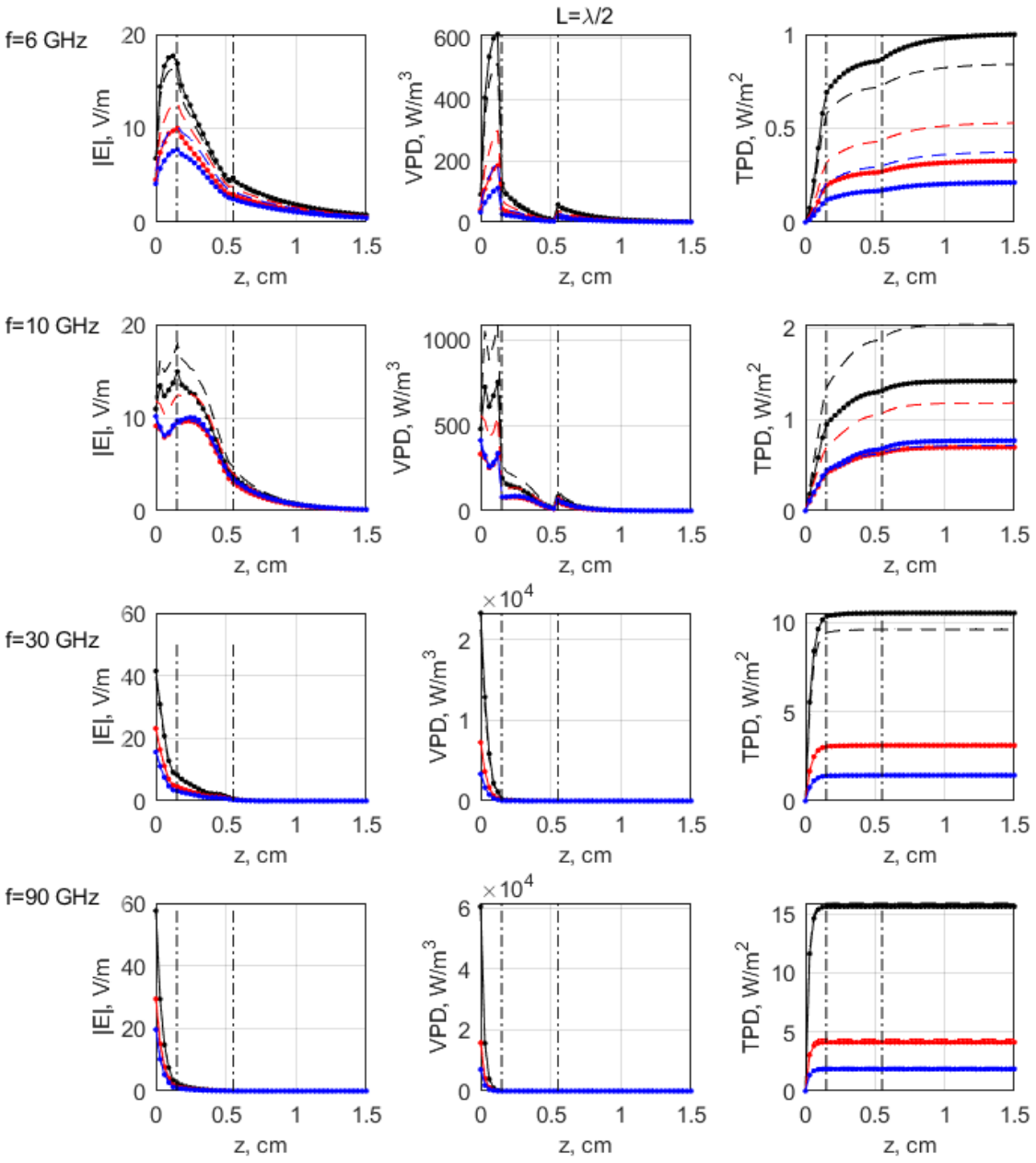

Fig. 8. Absolute value of electric field transmitted into the tissue (|*E*|, left), volume power density (*VPD*, center) and transmitted power density (*TPD*, right) vs. tissue depth for halfwave dipole ($L=\lambda/2$) above three-layered tissue.

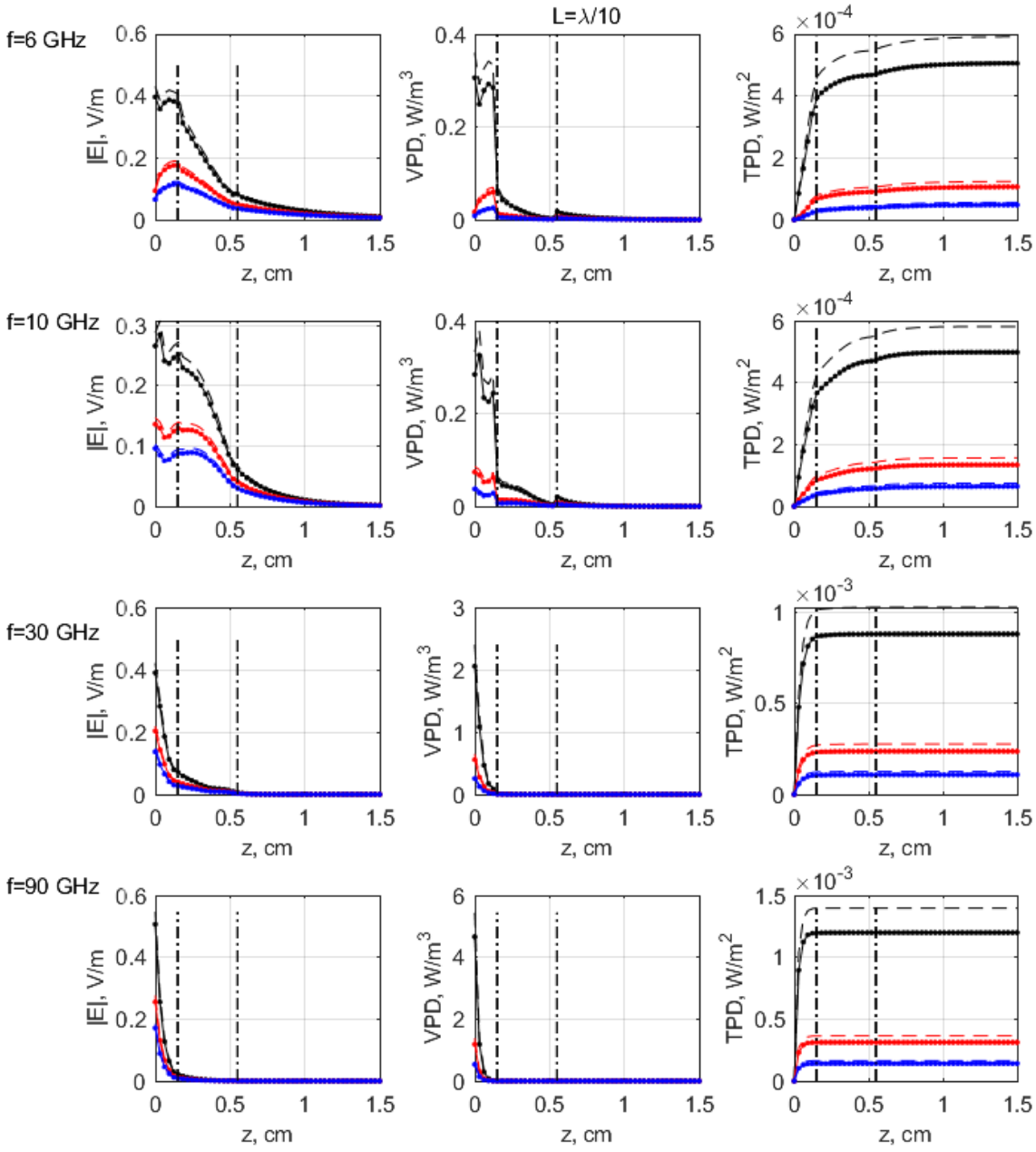

Fig. 9. Absolute value of electric field transmitted into the tissue (|*E*|, left), volume power density (*VPD*, center) and transmitted power density (*TPD*, right) vs. tissue depth for quarter-wavelength dipole ($L=\lambda/4$) above three-layered tissue.

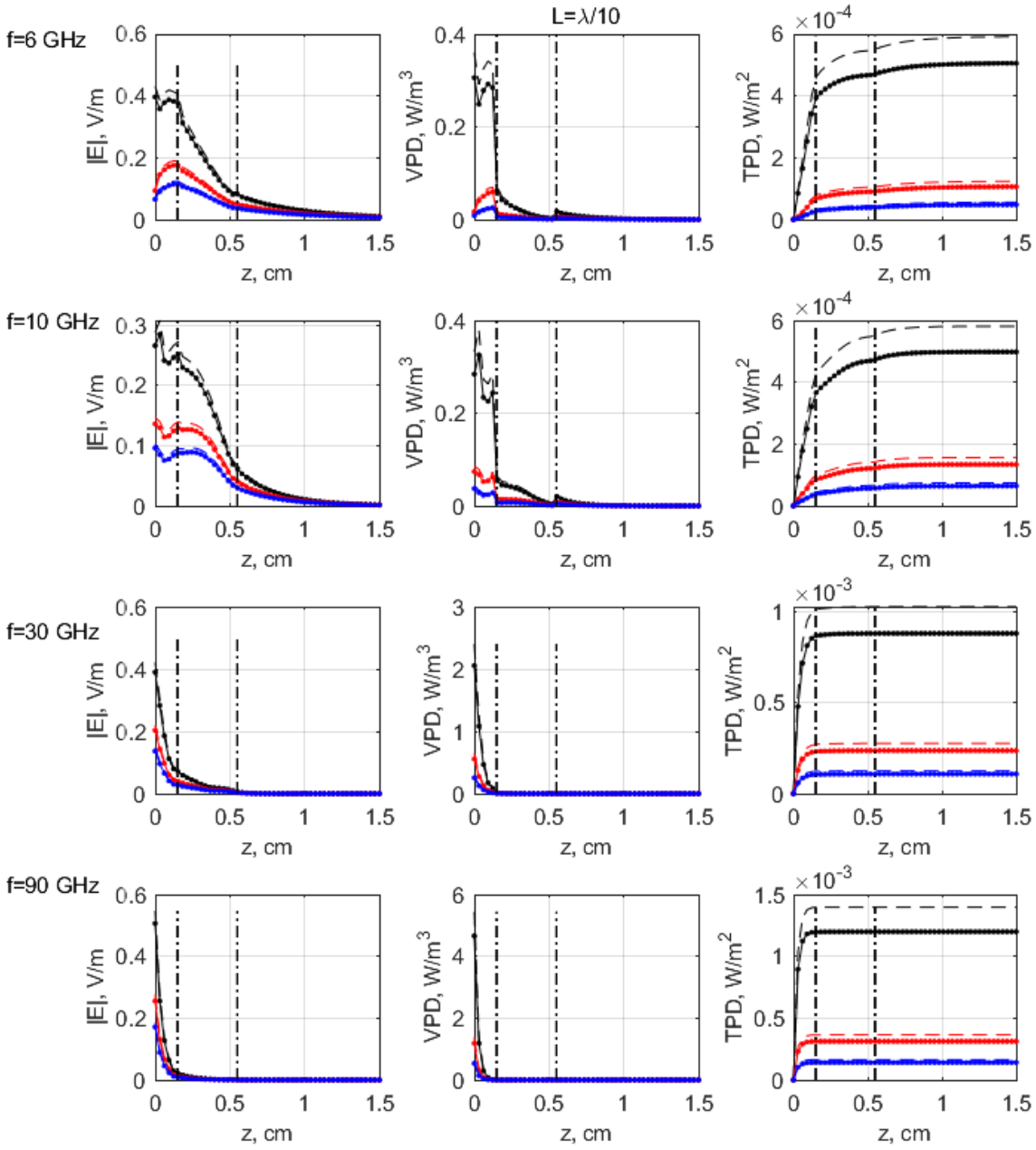

Fig. 10. Absolute value of electric field transmitted into the tissue (|*E*|, left), volume power density (*VPD*, center) and transmitted power density (*TPD*, right) vs. tissue depth for tenth-wavelength dipole ($L=\lambda/10$) above three-layered tissue.

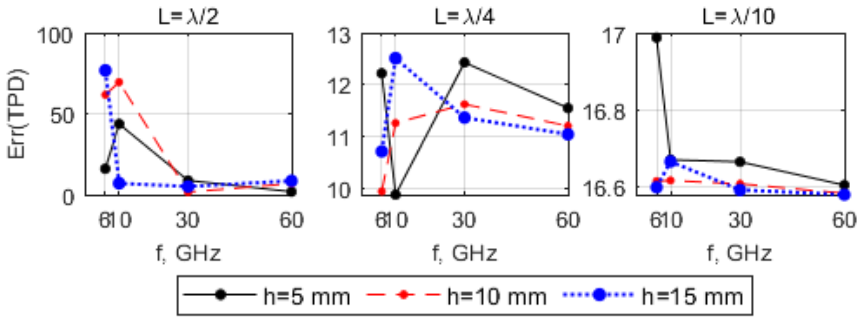

Fig. 11. Absolute relative error for *TPD* in three-layered body model computed as $Err(TPD) = |TPD_{num} - TPD_{ana}| / |TPD_{ana}|*100$. Subscripts *num* and *ana* denote *TPD* computed with numerical and analytical current solutions, respectively.

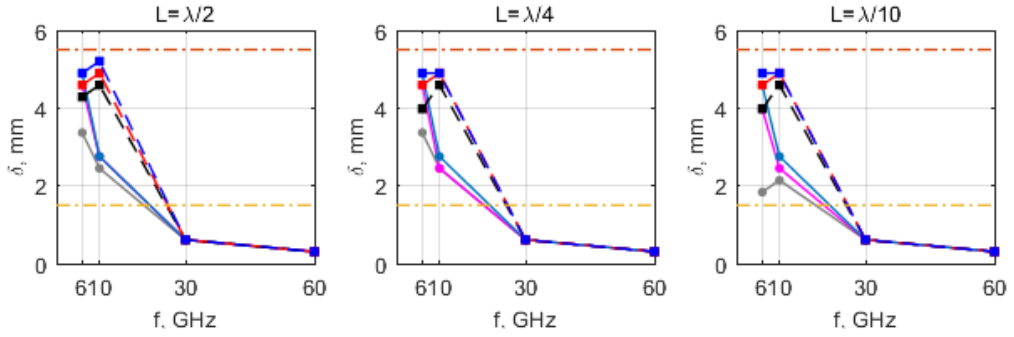

a) Skin-depth, δ for electric field values versus frequency

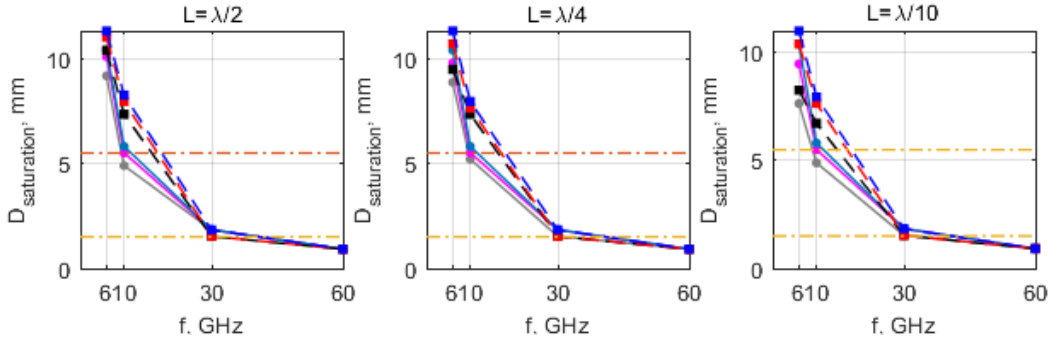

b) Saturation depth for *TPD* values versus frequency

Height, h	5 mm	10 mm	15 mm
Two-layer model	-•-	-•-	-•-
Three-layer model	-•-	-•-	-•-

Fig. 12. Electric field skin-depth (a) and *TPD* saturation depth (b) vs. frequency at three antenna heights: h=5 mm, h=10 mm and h= 15 mm. The yellow horizontal dotted line represents skin-muscle interface for two layered model and skin-fat interface for three layered model. The brown horizontal dotted line represents the fat-muscle interface for three layered model.

Fig. 11 depicts the relative absolute error between the analytical and numerical *TPD* solutions. The difference decreases as frequency and antenna-body distance increase. Number of tissue layers has negligible impact. The appreciable discrepancies between analytical/numerical results occur for L=λ/2 at frequencies 6 and 10 GHz.

C. Skin-depth and Saturation-depth

To further compare the results obtained for two-layer and three-layer body models for the same input parameter setup, i.e., the same combination of different antenna lengths, antenna heights and frequencies, the results for skin-depth and saturation-depth are given in Fig. 12.

It is worth noting that "skin" in "skin-depth" should not be mistaken for biological skin (here the 1st layer). The skin-depth (δ), as previously defined, is the distance in the tissue or some other material from the air-material interface at which electric field magnitude drops to 36% of its maximal value.

In this analysis, the saturation-depth ($D_{saturation}$) is defined as the distance in the tissue from the air-body interface at which

TPD reaches 98% of its maximal value.

At 6 and 10 GHz the skin-depth is in the 2nd tissue for both two-layer and three-layer models. The 2nd layer is muscle for two- and fat for three-layer model. The skin-depth at 30 and 60 GHz it is in skin tissue no matter the number of layers, antenna height and antenna length.

The saturation-depth for the two-layer model is in muscle tissue at 6 and 10 GHz and practically at skin-muscle interface at 30 GHz. As for the three-layer model the saturation-depth is in the muscle tissue at 6 and 10 GHz and at fat-skin interface at 30 GHz. The saturation-depth is in skin tissue at 60 GHz for both models. This does not depend on antenna-length.

IV. Concluding Remarks

The paper deals with an analytical/numerical approach to assess the transmitted field, volume power density (*VPD*) and transmitted power density (*TPD*) due to radiation of dipole antenna in front of planar multi-layered medium representing the human tissue. Such a model is described by skin, fat and muscle electrical properties on a given frequency. The influence of multilayer interface is considered via the corresponding Fresnel plane wave reflection/transmission approximation. Numerical procedures pertain to Galerkin-Bubnov Indirect Boundary Element Method (GB-IBEM) while analytical approach is based on the sinusoidal current distribution from a free space scenario. Some illustrative examples for the current distribution, transmitted field, volume power density and transmitted power density are given in the paper.

Conclusions drawn from the presented results can be summed up, as follows.

- Higher antenna-body distances will cause small increase in both skin-depth and saturation-depth.
- Moreover, the antenna height influence is weakening as the antenna length is reduced.
- Frequency variation has the biggest impact on skin-depth and saturation-depth. Increasing the frequency the impact of the antenna height, antenna length and number of layers becomes negligible.
- Discrepancies between the analytical and numerical approaches are the highest for half-wave dipole at 6 and 10 GHz. Increasing the frequency, the discrepancy falls to appx. 10%. The discrepancy decreases with the antenna length. This is important conclusion as the analytical approach is appreciably less demanding in terms of computational cost. Namely, the closed-form solution, i.e., analytical solution of current takes less computational time than the numerical solution via GB-IBEM method.

APPENDIX: TPD derivation from Poynting theorem

The Poynting integral theorem represents general conservation law of energy in the macroscopic electromagnetic field existing within a considered volume V and for the time-harmonic quantities can be written in the form:

$$\int_A \vec{S} * d\vec{A} = -j\frac{\omega}{2}\int_V \left(\mu\left|\vec{H}\right|^2 - \varepsilon\left|\vec{E}\right|^2\right) dV - \frac{1}{2}\int_V \sigma\left|\vec{E}\right|^2 dV + \frac{1}{2}\int_{V'} \sigma\left|\vec{E}'\right|^2 dV \quad \text{(A1)}$$

where $d\vec{A}$ is the outward drawn normal vector surface element, and complex Poyinting vector $\vec{S}$ is defined, as follows:

$$\vec{S} = \frac{1}{2}\left(\vec{E} \times \vec{H}^*\right) \quad \text{(A2)}$$

where *E* and *H* stand for the electric and magnetic field, respectively in the volume *V*. Note that *E'* stands for the field sources distributed over a volume *V'*, if they exist. As factor ½ appears *E* and *H* fields represent peak values, and it should be omitted for root-mean-square (rms) values.

Poynting theorem can be, for convenience, written with separated real part and imaginary part to emphasize different physical meaning:

$$Re\int_A \vec{S} * d\vec{A} = -\frac{1}{2}\int_V \sigma\left|\vec{E}\right|^2 dV + \frac{1}{2}\int_{V'} \sigma\left|\vec{E}'\right|^2 dV \quad \text{(A3)}$$

$$Im\int_A \vec{S} * d\vec{A} = -\frac{\omega}{2}\int_V \left(\mu\left|\vec{H}\right|^2 - \varepsilon\left|\vec{E}\right|^2\right) dV \quad \text{(A4)}$$

Thus, the real part of the integral over Poynting vector represents the total average power while the imaginary part of the integral over Poynting vector is proportional to the difference between average stored magnetic energy in the volume and average stored energy in the electric field. The total average power can, for example represent the radiated power by an antenna. In addition, the first volume integral in the right-hand side of (A3) represents power loss in the conducting medium.

The power loss defined in terms of the volume integral of power density can be rewritten by separating integration over an area from the line integration

$$P_L = \frac{1}{2}\int_V \sigma\left|\vec{E}\right|^2 dV = \frac{1}{2}\int_A \int_l \sigma\left|\vec{E}\right|^2 dAdl \quad \text{(A5)}$$

Now assuming the field not to vary appreciably over an area *A* (A5) simplifies into a line integral

$$P_L = \frac{1}{2}\int_l \sigma\left|\vec{E}\right|^2 Adl \quad \text{(A6)}$$

Finally, a dosimetric quantity referred to as transmitted power density (*TPD*) is simply obtained as ratio of power loss and the control area *A*

$$TPD = \frac{P_L}{A} \quad \text{(A7)}$$

and is given by the line integral

$$TPD = \frac{1}{2}\int_l \sigma\left|\vec{E}\right|^2 dl \quad \text{(A8)}$$

or using specific absorption rate (SAR) quantity it follows

$$TPD = \frac{1}{2}\int_l \rho \cdot SAR\, dl \quad \text{(A9)}$$

Line integrals in (A8) and (A9) are taken over the path perpendicular to the tissue surface.

REFERENCES

[1] IEEE, "IEEE Standard for Safety Levels with Respect to Human Exposure to Electric, Magnetic, and Electromagnetic Fields, 0 Hz to 300 GHz," *in IEEE Std C95.1-2019 (Revision of IEEE Std C95.1-2005/ Incorporates IEEE Std C95.1-2019/Cor 1-2019)*, pp. 1-312, 2019.

[2] ICNIRP, "Guidelines for Limiting Exposure to Electromagnetic Fields (100 kHz to 300 GHz)," *Health Physics*, vol. 118, no. 5, p. 483–524, 2020.

[3] S. Pfeifer et al., "otal Field Reconstruction in the Near Field Using Pseudo-Vector E-Field Measurements," *IEEE Transactions on Electromagnetic Compatibility*, vol. 61, no. 2, pp. 476-486, 2019.

[4] A. Hirata, D. Funahashi and S. Kodera, "Setting Exposure Gidelines and Product Safety Standards for Radio-Frequency Exposure at Frequencies above 6GHz: Brief Review," *Annals of Telecommunications*, vol. 74, pp. 17-24, 2019.

[5] B. Thors, D. Colombi, Z. Ying, T. Bolin and C. Törnevik, "Exposure to RF EMF From Array Antennas in 5G Mobile Communication Equipment," *IEEE Access*, vol. 4, pp. 7469-7478, 2016.

[6] D. Funahashi et al., "Averaging Area of Incident Power Density for Human Exposure from Patch Antenna Arrays," *IEICE Transactions on Electronics*, Vols. E101-C, no. 8, pp. 644-646, 2018.

[7] D. Poljak and V. Dorić, "On the Concept of the Transmitted Field and Transmitted Power Density for Simplifed Case of Hertz Dipole," in *EMC Europe 2020*, Rome, Italy, 2020..

[8] D. Poljak and V. Dorić, "Assessment of Transmitted Power Density due to Hertz Dipole Radiation using the Modified Image Theory Approach," in *28th International Conference on Software, Telecommunications and Computer Networks (SoftCOM)*, Split, Croatia, 2020.

[9] D. Poljak, A. Šušnjara and A. Džolić, "Assessment of Transmitted Power Density due to Radiation from Dipole Antenna of Finite Length, Part I: Theoretical Background and Current Distribution," in *29th International Conference on Software, Telecommunications and Computer Networks*, Hvar, Croatia, 2021.

[10] D. Poljak, A. Šušnjara and A. Džolić, "Assessment of Transmitted Power Density due to Radiation from Dipole Antenna of Finite Length Part II: Transmitted field, volume power density and transmitted power density," in *29th International Conference on Software, Telecommunications and Computer Networks*, Hvar, Croatia, 2021.

[11] A. Šušnjara, V. Dorić and D. Poljak, "Electric Field Radiated in the Air by a Dipole Antenna Placed above a Two-Layered Lossy Half Space: Comparison of Plane Wave Approximation with the Modified Image Theory Approach," in *26th International Conference on Software, Telecommunications and Computer Networks, SoftCOM*, Supetar, Croatia, 2018.

[12] A. Šušnjara, V. Dorić and D. Poljak, "Electric Field Radiated By a Dipole Antenna and Transmitted Into a Two-Layered Lossy Half Space: Comparison of Plane Wave Approximation with the Modified Image Theory Approach," in *2018 3rd International Conference on Smart and Sustainable Technologies (SpliTech)*, Split, Croatia, 2018.

[13] D. Poljak and K. El Khamlichi Drissi, Computational Methods in Electromagnetic Compatibility, Antenna Theory Approach versus Transmission Line Models, New York: John Wiley and Sons,, 2018.

[14] D. Poljak, Advanced Modeling in Computational Electromagnetic Compatibility,, New Jersey: John Wiley & Sons, Inc., 2007.

[15] C. Gabriel, "Compilation of the Dielectric Properties of Body Tissues at RF and Microwave Frequencies," Report N.AL/OE-TR- 1996-0037, Occupational and environmental health directorate, Radiofrequency Radiation Division, Brooks Air Force Base, Texas (USA), 1996.

[16] ITIS Foundation, "Copyright © 2010–2021 IT'IS Foundation," June 2019. [Online]. Available: [Online]. Available: https://itis.swiss/virtual-population/tissue-properties/database/..

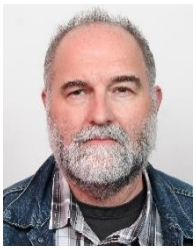

Dragan Poljak received his PhD in el. Eng. in 1996 from the Univ. of Split, Croatia. He is the Full Prof. at Dept. of Electron. and Computing, Univ. of Split. His research interests are oriented to computational electromagnetics (electromagn. compatibility, bioelectromagnetics and plasma physics). To date Prof. Poljak has published more than 160 journ. and 250 conf. papers, and authored some books, e.g. two by Wiley, New Jersey and one by Elsevier, St Louis. He is a Senior member of IEEE, a member of Editorial Board of Eng. Anal. with Boundary Elements, Math. Problems in Eng. And IET Sci. Measur. & Techn. He was awarded by several prizes for his achievements, such as National Prize for Science (2004), Croatian sect. of IEEE annual Award (2016), Technical Achievement Award of the IEEE EMC Society (2019) and George Green Medal from University of Mississippi (2021). From May 2013 to June 2021 Prof. Poljak was a member of the board of the Croatian Science Foundation. He is currently involved in ITER physics EUROfusion collab. and in Croatian center for excellence in research for tech. sciences. He is active in few Working Groups of IEEE/Internat. Committee on Electromagnetic Safety (ICES) Tech. Comm. 95 SC6 EMF Dosimetry Modeling.

Anna Šušnjara received her PhD degree in el. Eng. from the Univ. of Split, Croatia in 2021. She is a postdoc researcher at FESB, Univ. of Split. Her research interests include numerical modelling, uncertainty quantification and sensitivity analysis in computational electromagnetics.

Dr. Šušnjara was awarded with National Prize for Science in 2021 and Univ. of Split Prize for Science in 2022. In 2016 she received the best poster award at BioEM conference and spent one month at Politecnico di Torino as ACRI awardee in Young Investigator Training Program. She gave seminars/lectures about numerical modelling in computational electromagn. at several European academic institutions and tutorials at international scientific conferences. From 2015 until 2021 dr. Šušnjara was involved in ITER physics EUROfusion collab. In 2021 she joined a work group within IFMIF-DONES project. Dr. Šušnjara is a member of IEEE and BIOEM societies. She is currently a Vice President of Croatian chapter of IEEE EMC society.

To date, dr. Anna Šušnjara authored and co-authored 17 journ. and more than 35 conf. papers. She serves as a reviewer to seven journals and two conferences. A complete list of her publications can be found at: https://www.bib.irb.hr/pregled/znanstvenici/348056.

Ana Fišić received her bachelor and master's degrees in electrical engineering at Faculty of Electrical Engineering, Mechanical Engineering and Naval Architecture, Univ. of Split, Croatia. Her graduate education was focused on communication and information technology and in particular telecommunications and informatics.

During her master studies she did research on 5G technology with emphasis on internal dosimetry in gigahertz frequency range. She continued her professional development at Ericsson Nikola Tesla in Zagreb as a software developer in Java. Ana is currently working on 5G related projects as member of a Swedish CI team at Ericsson.